

# Journal Pre-proof

A unified mechanics theory-based model for temperature and strain rate dependent proportionality limit stress of mild steel

Noushad Bin Jamal M, C. Lakshmana Rao, Cemal Basaran



PII: S0167-6636(21)00020-X

DOI: <https://doi.org/10.1016/j.mechmat.2021.103762>

Reference: MECMAT 103762

To appear in: *Mechanics of Materials*

Received Date: 1 October 2020

Revised Date: 5 January 2021

Accepted Date: 7 January 2021

Please cite this article as: Jamal M, N.B., Rao, C.L., Basaran, C., A unified mechanics theory-based model for temperature and strain rate dependent proportionality limit stress of mild steel, *Mechanics of Materials* (2021), doi: <https://doi.org/10.1016/j.mechmat.2021.103762>.

This is a PDF file of an article that has undergone enhancements after acceptance, such as the addition of a cover page and metadata, and formatting for readability, but it is not yet the definitive version of record. This version will undergo additional copyediting, typesetting and review before it is published in its final form, but we are providing this version to give early visibility of the article. Please note that, during the production process, errors may be discovered which could affect the content, and all legal disclaimers that apply to the journal pertain.

© 2021 Published by Elsevier Ltd.

**Author Contributions:**

**Noushad Bin Jamal M, C. Lakshmana Rao, Cemal Basaran:** Conceptualization.; **Noushad Bin Jamal M, C. Lakshmana Rao, Cemal Basaran:** Methodology; **Noushad Bin Jamal M:** Software; **Noushad Bin Jamal M:** Validation; **Noushad Bin Jamal M, C. Lakshmana Rao, Cemal Basaran:** Formal Analysis; **Noushad Bin Jamal M, C. Lakshmana Rao, Cemal Basaran:** Investigation; **Noushad Bin Jamal M, C. Lakshmana Rao:** Resources; **Noushad Bin Jamal M, C. Lakshmana Rao, Cemal Basaran:** Data Curation; **Noushad Bin Jamal M:** Writing-Original Draft Preparation; **Noushad Bin Jamal M:** Writing-Review & Editing; **C. Lakshmana Rao, Cemal Basaran:** Supervision

Journal Pre-proof

# A unified mechanics theory-based model for temperature and strain rate dependent proportionality limit stress of mild steel

Noushad Bin Jamal M<sup>a</sup>, C. Lakshmana Rao<sup>a</sup>, and Cemal Basaran<sup>b</sup>

<sup>a</sup>Department of Applied Mechanics, Indian Institute of Technology, Madras600036.

<sup>b</sup>Civil, Structural and Environmental Engineering, University at Buffalo, State University of New York.

## Abstract

Strain rate and temperature dependent elastic limit of mild steel is investigated by developing a dislocation incipient motion-based proportionality limit stress model. Temperature effect on strain energy of an edge dislocation is modeled by using unified mechanics theory. Unified mechanics theory-based index, called thermodynamic state index, is used to model thermally assisted degradation of strain energy. Kinetic energy due to thermal vibrations is added to the kinetic energy of an accelerating dislocation. It is shown that, prior to the onset of observable plastic slip at the macrolevel, dislocation incipient motion is dominated by inertial effects within the elastic limit, rather than drag controlled mechanisms, that are normally observed in the post-yield response of metals. A new model for temperature and strain rate dependent critical shear stress is derived. Validation of the derived model with experimental data and comparison of model predictions with Johnson-Cook model predictions for mild steel at zero plastic strain shows that the micromechanics of rate and temperature dependence of the elastic response of mild steel involve inertia dominated mechanism at higher temperatures.

Keywords: Dislocation; Proportionality limit stress; Temperature dependence; Strain rate; Unified mechanics theory;

## 1. Introduction

Strain rate and temperature dependence of proportionality limit stress (initial yield point) in metals are very well known (Campbell and Ferguson, 1970). In metals, proportionality limit represents a limiting point, beyond which the deformation is inelastic. As an example, the strain rate dependence of proportionality limit stress for mild steel is highlighted at zone A, as shown in Fig. 1. Elastic deformation in metals and other materials can be non-proportional as well. However, on the basis of mechanical experiments, mild steel is observed to have a proportional

behavior between stress and strain, before the onset of plastic yielding. High strain rate mechanical tests (within a strain rate of  $10^4$  1/s) are performed using a dynamic testing machine such as Split Hopkinson Pressure Bar (SHPB), dynamic hydraulic testing machine, or drop weight tester. Experimental results shown in Fig. 1., are obtained by conducting tests on cylindrical specimens, using a dynamic hydraulic testing machine (Campbell and Ferguson, 1970). Even though a constant strain rate is said to be ensured during experiments, the strain rate will accelerate from zero to a constant value. Hence, during the initial stages of high-speed deformation in mild steel, elastic deformation involves inertial effects, leading to an increase in proportionality limit stress, as shown in Fig. 1. On the other hand, the effect of temperature in mild steel is reverse, in preheated specimens (Campbell and Ferguson, 1970). As the specimen temperature is increased by preheating, proportionality limit stress is reduced for a given strain rate (Campbell and Ferguson, 1970). Therefore, it is relevant to study the strain rate and temperature dependent elastic response of metals, like mild steel. For modeling the behavior of crystalline materials like metals, several macro-level (length scale in the order of mechanical experiments) models (Johnson and Cook, 1983), crystal level (length and time scales are of the order of nanoseconds and micrometers respectively) models (Pellegrini, 2010; Voyiadjis and Abed, 2005) and atomic level (length and time scale is of the order of femtoseconds and nanometers respectively) models (Brandl et al., 2009) are available in the literature. Curve fitting of macrolevel models to experimental data (Johnson and Cook, 1983) gives better prediction than lower length scale models. However, such empirical curve-fit models do not explain the physics behind temperature and strain rate dependency of proportionality limit stress (onset of yielding). Computational domain length and time scales in atomic-level studies are of the order of nanometres and femtoseconds (Brandl et al., 2009), respectively. Hence, using an atomic level model to predict proportionality limit stress at experimental level length and times scales is computationally very expensive.

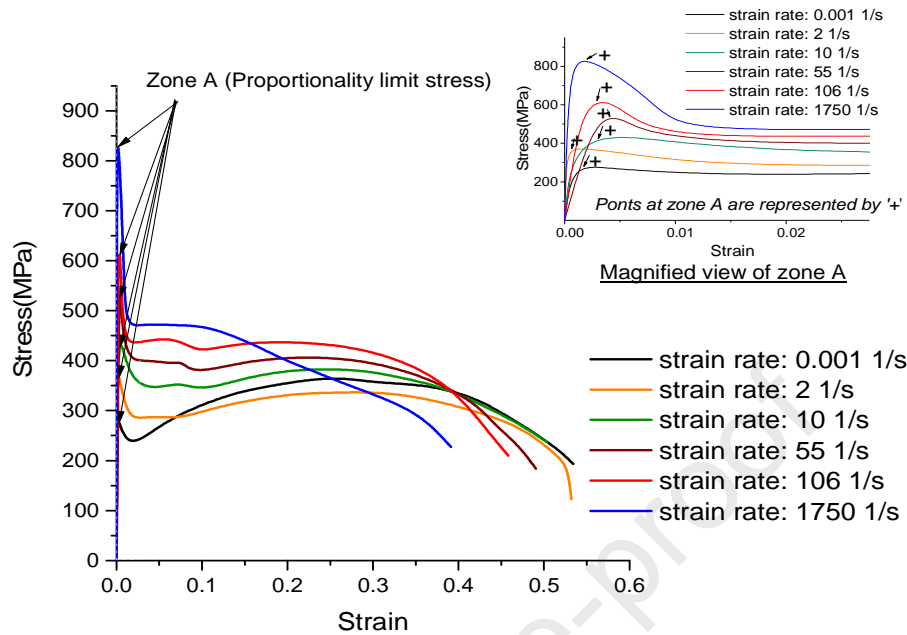


Fig. 1. Stress-strain plots for a wide range of strain rates in tensile loading experiments on mild steel (Blazynski, 1987)

Physics of elastic response of metals is explained better, by micromechanics-based models such as dislocation models (Hirth and Lothe, 1983). Distribution, geometry, incipient motion, density, etc., of inherent defects such as inclusions, voids, and dislocations play a major role in the elastic behavior of metals (Hirth and Lothe, 1983; Ni, 2005). Elastic response of dislocation and their strain energy-based critical slip resistance are well known in the field of dislocation mechanics since 1934 (Eshelby, 1953; Hirth and Lothe, 1983; Polanyi, 1934). However, strain rate dependent elastic response of metals as highlighted in Fig. 1., as an example, has not been completely explained by dislocation models. Nevertheless, it is generally assumed that the dislocations are immobile during elastic deformations.

Molecular dynamics could simulate the mechanics of dislocation incipient motion prior to the onset of observable plastic slip, under high strain rate and temperature (Brandl et al., 2009). From atomic level numerical studies, it is reported in the literature (Brandl et al., 2009) that the dislocation motion is delayed and the number of slips is increased at higher strain rates and lower temperatures. Load dependent delayed response at the atomic level can be due to drag controlled mechanisms. However, the dislocation drag mechanism is dissipative and hence they are insignificant within the proportionality limit. Other hypotheses on the rate-dependent elastic limit

of metals are, the interaction of dislocations with obstacles while in motion, dislocation generation by Frank-Read sources, and decelerated dislocation annihilation. But, increasing dislocation density causes more plastic slip, instead of elastic deformation at the macro-level (Suzuki et al., 2013; Taylor, 1992). Hence, these mechanisms reported in the literature could capture the post-yield behavior of metals under high strain rates. However, such hypotheses may not be fully validated before the onset of observable plastic slip (Ansart and Dornmeval, 1989), which is the focus of this study. In this study, we attempt to investigate the rate and temperature dependent proportionality limit stress of mild steel (Campbell and Ferguson, 1970), by applying dislocation inertia as a non-dissipative probable mechanism.

Fig. 1 shows that the proportionality limit of mild steel is highly dependent on the strain rate. The literature on temperature and strain rate dependence of mild steel (Campbell and Ferguson, 1970) and other metals (Blazynski, 2012) shows that the effects of strain rate and temperature are not only coupled but the effect of one on the proportionality limit stress, is opposite to the other. It is reported in the literature (Suzuki et al., 1991) that, dislocation annihilation is accelerated at high temperatures. There are many experimental and numerical models (Johnson and Cook, 1983) reported in the literature, to capture the post-yield response of metals, successfully. However, until recently, there has been no proper attempt to model coupled thermal and rate dependence of the elastic response of metals, based on their micro-mechanisms.

The main goal of the present work is to model the temperature and strain rate dependent elastic limit stress in mild steel, using a semi-infinite dislocation model. To achieve the goal, in the first stage, we introduce an edge dislocation model in a continuum framework. Using the dislocation model, we write the Lagrangian of the dislocation and apply Hamilton's principle to get the critical stress at dislocation incipient motion. Considering non-dissipative mechanisms prior to the onset of observable plastic slip (within elastic response), strain energy of dislocation and the kinetic energy at the incipient motion of dislocation, are presented and Lagrangian of the dislocation is written. Strain energy is derived based on elasticity theory as detailed in section 2. In the second stage of this work, temperature dependence is introduced in the strain rate dependent governing equation. Temperature is changed in the test specimens by preheating the samples, before the mechanical tests. Since the current focus is on the modeling of proportionality limit stresses (at negligible plastic strains), we do not consider any plastic dissipation processes, within the proportionality limit stresses. By heating the samples, atomic

vibrations change and the dislocation starts annihilating by a decrement in strain energy of dislocations. Such existence of dislocations at a given temperature to annihilated state can be modeled by introducing a life index, using unified mechanics theory (Basaran, 2020; Bin Jamal M. et al., 2020), called Thermodynamic State Index, TSI. Unified mechanics theory is the unification of the second law of thermodynamics and Newton's laws of motion. Unified mechanics theory introduces an additional axis, called Thermodynamic State Index, TSI (Basaran, 2020; Bin Jamal M. et al., 2020) to space-time coordinate axes. The life axis, TSI is a function of thermodynamic quantity, called entropy. TSI axis coordinate defines the system in thermodynamic space. This theory has been mathematically proven, experimentally validated for different materials, and reported in the literature (Basaran, 2020). Temperature dependence of strain energy of dislocation is formulated by using the unified mechanics theory (Basaran, 2020; Bin Jamal M. et al., 2020). Section 2 presents the application of the Thermodynamic State Index in deriving temperature dependent strain energy of a dislocation. The concept of inertia and the mathematical form of kinetic energy are detailed in section 3. Temperature dependence of kinetic energy at the microlevel is expressed by introducing functional dependence of accelerating dislocation mass with the vibrational characteristics of associated atoms, as detailed in section 3. Lagrangian of the accelerating dislocation system in the elastic region of loading is expressed in its functional form as detailed in section 4. In section 5, Hamiltonian formalism is used to derive a temperature dependent threshold stress and subsequently, the unknown terms are derived. Verification of the proposed model is done by comparing with test data for a wide range of temperature and strain rate, as detailed in section 6. Since, a consistent ratio between the initial yield point and proportionality limit stress is observed from the experimental results on mild steel (Campbell and Ferguson, 1970), the derived model is used to predict lower yield stress values, at different strain rates and then compared with well-known Johnson-Cook model (Johnson and Cook, 1983) predictions at zero plastic strain, as detailed in section 7. Major observations on the procedure, model structure, and its nature of predictions in comparison with experimental observations (Blazynski, 2012; Campbell and Ferguson, 1970) and the Johnson-Cook model (Johnson and Cook, 1983) are discussed in section 8 and major conclusions are listed in section 9.

## **2. Strain energy of an edge dislocation**

In this section, we introduce a time-dependent form of strain energy of a semi-infinite edge dislocation model to explain the strain rate-dependent elastic response of metals such as zone A shown in Fig. 1. The physical background of dislocation formation and strain energy of dislocation is, as follows. Dislocations are generated during the crystallization of metallic materials. Hence, the equilibrium of dislocation at rest conditions is attained through the creation of a strain energy field around the dislocation. A schematic diagram of idealized equilibrium geometry, including the geometric features of the edge dislocation, is shown in Fig. 2. A two-dimensional representation of atomic stacking is shown in red color, in Fig. 2. Origin of the coordinate axes X and Y in Fig. 2., is the center of a semi-infinite edge dislocation. The disregistry between atoms at each point along X direction is represented by  $\delta(x)$ . At each point along X-axis, the disregistry,  $\delta$  represents infinitesimal Burgers vector and summation of all the disregistry give the Burgers vector,  $b$ . Hence, far away from the dislocation, disregistry,  $\delta$  is zero. Local displacements (at  $x = x'$ ) between the atoms are represented by  $u$ . A magnified view of the displacement  $u$  is shown in Fig. 2. The classical approach (Hirth and Lothe, 1983) considers this strain energy to calculate the resisting force of metallic crystal at the onset of dislocation incipient motion. In this study, we consider a straight edge dislocation in a semi-infinite domain as shown in Fig. 2. An edge dislocation is represented as distributed disregistries around the dislocation, as shown in Fig. 3. Local trace of the disregistries shown in Fig. 3., is used to show the gradient of disregistry. It is shown in Fig. 3., that at the center of dislocation (at  $x=0, y=0$ ), the disregistry is maximum and equals to the magnitude of Burgers vector,  $b$ , however, disregistry asymptotically reduces to zero at a distance,  $+L$  and  $-L$ , which are considered as the bounds of the domain. A Burgers vector at a given time is represented by the summation of all these disregistries (Hirth and Lothe, 1983) as follows,

$$\int_{-\frac{b}{2}}^{\frac{b}{2}} d\delta(x', t) = \int_{-L}^{+L} \delta'(x, t) dx = \delta(+L, t) - \delta(-L, t) = \frac{b}{2} - \left(-\frac{b}{2}\right) = b \quad (1)$$

where  $d\delta$  and  $\delta'$  are the disregistry and the gradient of local disregistry, as shown in Fig. 3. The magnitude of Burgers vector is represented by 'b' for the infinitely large domain, bounded by  $[-L, +L]$ , where  $L$  tends to infinity in the domain, as shown in Fig. 2.



Fig. 2. Schematic representation of geometric parameters of an idealized edge dislocation model

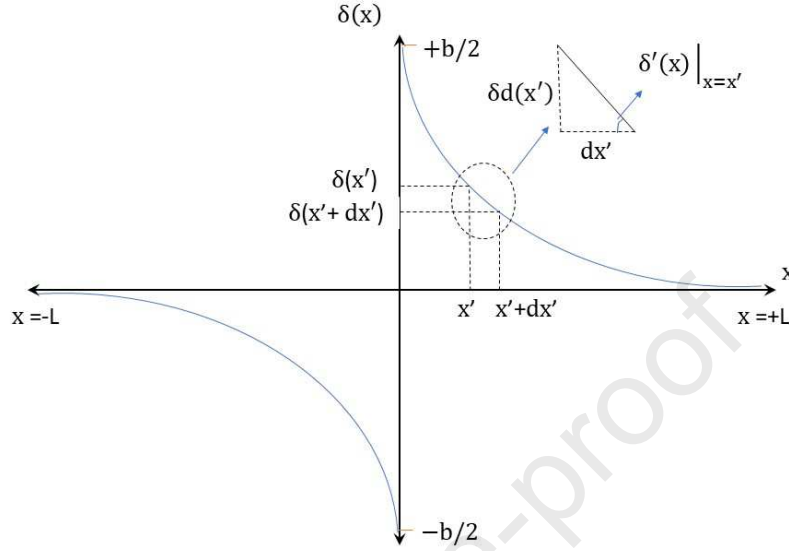


Fig. 3. Trace of disregistry along the x-axis

where,  $\delta(x, t)$  is the infinitesimally small disregistry. Upon integration of the equation (4) over the domain,  $-L$  to  $+L$ , we get the total work done as follows,

$$\delta W^E = \int_{-L}^L \int_{-\frac{b}{2}}^{\frac{b}{2}} \frac{G}{2\pi(1-\nu)} \frac{d\delta(x', t)}{(x-x')} \delta(x, t)|_{t=0} dx \quad (5)$$

Using equation (1) in equation (5) and integrating by parts, we get the following equation,

$$\delta W^E = -\frac{G}{2\pi(1-\nu)} \int_{-L}^L \int_{-L}^L \delta'(x, t) \delta'(x', t) \ln(x-x') dx dx' \quad (6)$$

We assume that the dislocation geometry is not distorted at rest and also during the incipient motion. However, under extreme dynamic events, such as ultra-high strain rate deformation, dislocation geometry can get distorted by the interaction of neighbouring dislocations, cross-slip mechanism, etc. A separate study shall be done to investigate the change in geometry of dislocation core, under extreme dynamics. The focus of this study is limited to model the incipient motion of single dislocation and derive the proportionality limit stress, within a

benchmark strain rate of  $10^4$  1/s and hence, the above assumption on fixed core geometry is valid. The total strain energy required to nullify the formation of an edge dislocation system is given as follows,

$$U_T^E(\delta) = \frac{1}{2} \int_{-L}^L \int_{-\frac{d}{2}}^{\frac{d}{2}} \int_{-L}^{+L} \sigma_{xy} \varepsilon_{xy} dx dy dz \quad (7)$$

where,  $U_T^E$  represents the total strain energy. Integral bounds of equation (7) are shown in Fig. 2. Inter-planar distance between the slip planes is represented by 'd' and the shear strain,  $\varepsilon_{xy}$  represents the shear strain and  $\sigma_{xy}$  is the shear stress to be applied to counteract the formation-energy around the dislocation. Hence,  $\sigma_{xy}$  in equation (3) and equation (7) are similar. From Fig. 2 and Fig. 3, we write the shear strain,  $\varepsilon_{xy}$  as follows,

$$\varepsilon_{xy} = \frac{2\delta(x, t)}{d} \quad (8)$$

The assumption on undistorted edge dislocation geometry may not be valid during a plastic slip, under ultra-high strain rates. However, it is very important to emphasize that, we are only interested in the incipient motion of dislocations, prior to attaining a terminal velocity for the plastic slip. Since the local vibrations of the atoms are governed by the energy levels of atoms, the geometrical aspect of dislocation is governed by the energy levels of atoms. Temperature variation is one of the reasons to alter the geometry of the dislocations. The stability of the geometry of dislocation is assumed here, only below a critical temperature. Hence, using equation (3), equation (7), equation (8) and with the assumption of unaltered dislocation geometry at a given temperature, the total strain energy per unit length of dislocation is written as follows,

$$U^E(\delta) = \frac{G}{2\pi(1-\nu)} \int_{-L}^{+L} \left[ \int_{-L}^L \left\{ \frac{1}{(x-x')} \frac{d\delta(x', 0)}{dx'} dx' \right\} \right] \delta(x, t) dx \quad (9)$$

The integral form of strain energy of an edge dislocation, given in equation (9), does not explicitly represent temperature dependency. However, one can define the material parameters, G and  $\nu$  as a function of temperature. In this study, we use the unified mechanics theory to model the temperature dependency of strain energy given in equation (9) and incorporate thermally

assisted dislocation annihilation process. Details of the functional dependency of equation (9) with temperature, are given in the succeeding sections.

### 3. Kinetic energy of a mobile edge dislocation under thermo-mechanical loading

In this section, we explain the physical background of inertia of dislocation at incipient motion and represent the kinetic energy, as follows. When a metallic material is subjected to mechanical loading, the atoms move and attain new equilibrium positions at a deformed configuration. These new equilibrium positions of the atoms in the bulk material represent strain. Once the motion of the atoms is initiated, the dislocations formed by the atoms also have to move. The inertia involved in the onset of mobilization of dislocation incipient motion from a state of rest to reach a terminal state is governed by the applied strain rate (Orowan, 1934). Hence the motion of dislocations during mechanical deformation is quantified in terms of the kinetic energy of dislocation, in addition to the mobilization resistance due to the strain energy, given in equation (9).

The incipient motion of dislocation is governed by the incipient motion of surrounding atoms. Hence, the inertia of dislocations is associated with a dislocation mass. Inertial mass is a function of dislocation geometry. In the current formulation, we represent the inertial mass of an infinitesimally small disregistry, as follows,

$$dm = \alpha \rho_m \delta' dx dy \quad (10)$$

where  $dm$  represents the mass per unit length of disregistry. The mass density of the material is represented by  $\rho_m$  and the factor,  $\alpha$  represents a mass factor for calculating the associated mass in the accelerated motion of a dislocation. Hence, we write the kinetic energy of dislocation incipient motion during the elastic deformation of the bulk material as follows,

$$K_E(\delta, t) = \int_{-L}^{+L} \int_{-\frac{d}{2}}^{+\frac{d}{2}} \frac{1}{2} \alpha \rho_m \delta'(x, t) \left| \frac{\partial \delta}{\partial t} \right|^2 dy dx \quad (11)$$

Using equation (1) and equation (11), we get the following equation,

$$K_E(\delta, t) = \frac{1}{2} \alpha \rho_m d \int_{-L}^{+L} \delta'(x, t) \left| \frac{\partial \delta}{\partial t} \right|^2 dx \quad (12)$$

where,  $K_E$  represents the kinetic energy due to mechanical loading. Under thermal loading, the kinetic energy of the dislocation has an additional part. Kinetic energy induced by the thermal vibration of atoms associated with the same dislocation is represented by a mass factor,  $\alpha$  in equation (12), and can be written as follows,

$$K_{\theta}(\delta, \theta) = \frac{1}{2} \alpha \rho_m d \int_{-L}^{+L} \delta'(x, t) |\bar{v}_{\theta}|^2 dx \quad (13)$$

where,  $\bar{v}_{\theta}$  represents the mean vibrational velocity of atoms for a given thermal loading. Hence, the total kinetic energy can be written as the summation of equation (12) and equation (13), as follows,

$$\sum K_E = \frac{1}{2} \alpha \rho_m d \int_{-L}^{+L} \delta'(x, t) \left( \left| \frac{\partial \delta}{\partial t} \right|^2 + |\bar{v}_{\theta}|^2 \right) dx \quad (14)$$

In equation (14), the rate of change of mean position of atomic vibration is represented by mean vibrational velocity,  $\bar{v}_{\theta}$ . Hence the equation (14) can be represented in terms of the mean position of atoms as follows,

$$\sum K_E = \frac{1}{2} \alpha \rho_m d \int_{-L}^{+L} \delta'(x, t) \left( \left| \frac{\partial \delta}{\partial t} \right|^2 + \left( \frac{\partial \bar{x}}{\partial t} \right)^2 \right) dx \quad (15)$$

where,  $\bar{x}$  represents the mean position of atoms due to thermal vibration. Since the value of disregistry,  $\delta$  and the mean position of atoms,  $\bar{x}$  are evaluated for the dislocation, we represent the equation (15) in terms of a dimensionless multiplier,  $\varphi$  for the disregistry,  $\delta$  as follows,

$$\sum K_E = \frac{1}{2} \alpha \rho_m d \int_{-L}^{+L} \varphi \delta'(x, t) \left( \left| \frac{\partial}{\partial t} (\varphi \delta) \right|^2 \right) dx \quad (16)$$

where,  $\varphi$  represents a dimensionless multiplier for the disregistry,  $\delta$ , to account for the heat-induced kinetic energy of atoms, surrounding the dislocation. Under thermal loading (by preheating the sample) atomic vibration amplitudes change (Owen and Evans, 1967). Hence, due to eventual change in strain energy, bounds of a dislocation geometry changes. Consequently, the increment in temperature reduces dislocation mass. Hence, the equation (16) is represented in terms of the mean amplitude of atomic vibration as follows,

$$\sum K_E = \frac{1}{2} \alpha_\theta(\bar{u}_\theta) \rho_m d \int_{-L}^{+L} \delta'(x, t) \left( \left| \frac{\partial \delta}{\partial t} \right|^2 \right) dx \quad (17)$$

where, the dimensionless factor,  $\alpha_\theta^3$  in equation (16) is represented in equation (17) by a dimensionless function,  $\alpha_\theta(\bar{u}_\theta)$  in terms of the mean amplitude of atomic vibration,  $\bar{u}_\theta$ , for a given temperature,  $\theta$ . In equation (17) the parameter,  $\alpha_\theta$  represents temperature dependent mass factor.

#### 4. Temperature-dependent model using unified mechanics theory

Under different test temperatures, both the strain energy and kinetic energy levels of a dislocation, changes. Temperature dependency of the kinetic energy of an edge dislocation under incipient motion and thermally induced vibrations is presented in section 3. However, strain energy of an edge dislocation, presented in section 2, is independent of temperature. Thermally-induced dislocation annihilation (Suzuki et al., 1991) is a well-known mechanism. In this study, we attempt to model preheating induced dislocation annihilation as a process of degradation, along a life axis called Thermodynamic State Index (TSI) axis. According to the laws of unified mechanics theory (Basaran, 2020), Thermodynamic State Index (TSI) axis represents thermodynamic space in addition to the Newtonian space-time axes. Using unified mechanics theory (Basaran, 2020), thermally induced degradation of strain energy of dislocation at a given temperature, in comparison with the strain energy at a reference temperature, is written as follows,

$$U'^E = (1 - \Phi(\theta))U^{0E} \quad (18)$$

where,  $U'^E$  is the strain energy of dislocation at a given temperature and  $U^{0E}$  is the strain energy at a reference temperature. The TSI is represented by  $\Phi$ , which starts at zero and progresses to one (Basaran, 2020; Bin Jamal M. et al., 2020). The functional form of TSI (Basaran, 2020) is given as follows,

$$\Phi = \Phi_c \left( 1 - \exp \left( -\Delta s(\theta) \frac{m_s}{R} \right) \right) \quad (19)$$

where,  $\Phi_c$ ,  $m_s$  and  $R$  represents the critical value of TSI, molar mass of the material, and gas constant, respectively. The total change in entropy of the dislocation structure due to change in test temperature is represented by  $\Delta s(\theta)$ . The evolution of TSI from zero to one depicts

thermally assisted dislocation annihilation process, in equation (18). Temperature-dependent model for change in entropy in equation (19), is presented in the succeeding section. Hence, strain rate and temperature dependency of dislocation incipient motion is incorporated in kinetic energy and strain energy equations. To derive the critical stress at the incipient motion of a dislocation, the total Lagrangian of dislocation is written using the above strain energy equation and kinetic energy equations, and the resulting form of functional is minimized, as detailed in the following section.

## 5. The resistance of motion of dislocation and representation of total Lagrangian

Classical Lagrangian describes conservative systems, however, an extension of the Lagrangian can be used to model nonconservative forces such as friction. In this study, no nonconservative forces are considered and the deformation within the proportionality limit is non-dissipative. Dissipation due to temperature change is included in a separate section, which takes care of the initial state of dislocation (before the mechanical testing) strain energy in a given preheated sample. Hence, the classical Lagrangian represents the deformation process of a given sample without any nonconservative forces. Externally applied energy,  $W_{\text{Tot}}(\delta)$  at the incipient motion of an edge dislocation is balanced by the work done by internal restoring force,  $F_b^T(\delta, \dot{\delta}, \theta, \zeta_i)$ . At the incipient motion of edge dislocation, the internal restoring force resists the creation of new discontinuity in stacking and annihilation of the existing stacking fault. The restoring force,  $F_b^T$  in moving the edge dislocation, is stored as potential energy at the incipient motion. This restoring surface energy is called generalized stacking fault energy,  $\gamma^T$  (Vitek, 1968). We consider the formal interpretation of stacking fault energy (Vitek, 1968) to derive the resisting surface force as the gradient of stacking fault energy,  $\gamma^T$ . Hence, the balance of force can be written (Vitek, 1968) as follows,

$$F_b^T(\delta, \dot{\delta}, \theta, \zeta_i) + \nabla[\gamma^T(\delta, \dot{\delta}, \theta, \zeta_i)] = 0 \quad (20)$$

where,  $\zeta_i$  represents a set of all other internal variables of the surface energy functional. Classical Lagrangian has the following form,

$$\mathcal{L} = \sum K_E - \sum V \quad (21)$$

where,  $\mathcal{L}$  is the Lagrangian, and  $\sum K_E$ ,  $\sum V$  represents the total kinetic energy and total potential energy of dislocation at incipient motion, respectively. Hence, substituting the equation (9), equation (18), equation (17), and equation (20) in equation (21), we get the following form of Lagrangian of the system,

$$\begin{aligned} \mathcal{L} = & \frac{1}{2} \alpha_\theta \rho_m d \int_{-L}^{+L} \delta'(x, t) \left( \left| \frac{\partial \delta}{\partial t} \right|^2 \right) dx + \int_{-L}^L \gamma^T(\delta(x, t), \hat{\delta}, \theta, \zeta) dx \\ & - \frac{G(1-\Phi)}{2\pi(1-\nu)} \int_{-L}^{+L} \left[ \int_{-L}^L \left\{ \frac{1}{(x-x')} \frac{d\delta(x', 0)}{dx'} dx' \right\} \right] \delta(x, t) dx \end{aligned} \quad (22)$$

Equation (22) involves kinetic energy and potential energy terms of dislocation at incipient motion, in their integral form. The following section is detailed with the application of Hamiltonian on equation (22), to get a threshold value of resistance of dislocation at its incipient motion.

## 6. Temperature-dependent threshold stress formulation

### 6.1. Critical resistance of edge dislocation at incipient motion

Hamilton's principle is applied to the action integral given in equation (22), to get the critical resisting force on an edge dislocation at its incipient motion. According to Hamilton's principle, the stationary path of an action integral in the present case can be mathematically represented as follows,

$$\int_{t_1}^{t_2} \left[ \frac{\partial \mathcal{L}}{\partial \delta} - \frac{d}{dt} \left( \frac{\partial \mathcal{L}}{\partial \dot{\delta}} \right) \right] \delta \delta = 0 \quad (23)$$

The validity of the above integral form shall hold for even the smallest possible domain. Hence, equation (23) can be written as follows,

$$\frac{\partial \mathcal{L}}{\partial \delta} - \frac{d}{dt} \left( \frac{\partial \mathcal{L}}{\partial \dot{\delta}} \right) = 0 \quad (24)$$

Surface energy,  $\gamma^T$  required to move a dislocation from one place to the other inherently involves dislocation annihilation and generation process. Hence, equation (24) applied on the surface energy term,  $\gamma^T$  represents the net force required to move the dislocation. In the present case, we

introduce this resisting force as given in equation (20), which can be derived by using surface energy,  $\gamma^T$  and equation (24), as follows.

$$\frac{\partial}{\partial \delta} \left[ \int_{-L}^L \gamma^T(\delta(x, t), \dot{\delta}, \theta, \zeta) dx \right] - \frac{d}{dt} \left( \frac{\partial}{\partial \dot{\delta}} \left[ \int_{-L}^L \gamma^T(\delta(x, t), \dot{\delta}, \theta, \zeta) dx \right] \right) = -b * \sigma_{DCS_\theta} \quad (25)$$

where,  $\sigma_{DCS_\theta}$  represents temperature dependent threshold shear stress required for a dislocation to move. The negative sign on the right-hand side of the equation (25) represents the reaction force that has taken its form from equation (20). To reduce the complexity of derivation, we consider that during the elastic deformation, dislocation is stable for a given temperature, below an annihilation threshold. Hence, for a given temperature, the movement of dislocation is considered to be unaltering the strain energy. This assumption brings a condition that the gradient of disregistry is constant throughout the acceleration process of an edge dislocation. Therefore, from equation (17) and equation (24), we get the following,

$$\frac{\partial}{\partial \delta} \left( \sum K_E \right) - \frac{d}{dt} \left( \frac{\partial}{\partial \dot{\delta}} \left( \sum K_E \right) \right) = -\alpha_\theta \rho_m d \int_{-L}^{+L} \delta'(x, t) \frac{\partial^2 \delta(x, t)}{\partial t^2} dx \quad (26)$$

Hence, from equation (22), equation (24), equation (25), and equation (26), we get the following equation,

$$\begin{aligned} b * \sigma_{DCS_\theta} = & \alpha_\theta \rho_m d \int_{-L}^{+L} \delta'(x, t) \frac{\partial^2 \delta(x, t)}{\partial t^2} dx + \frac{G(1 - \Phi)}{2\pi(1 - \nu)} \int_{-L}^{+L} \left[ \int_{-L}^L \left\{ \frac{1}{(x - x')} \delta' dx' \right\} \right] dx \\ & - \frac{G}{2\pi(1 - \nu)} \frac{\partial \Phi}{\partial \delta} \int_{-L}^{+L} \left[ \int_{-L}^L \left\{ \frac{1}{(x - x')} \frac{d\delta(x', 0)}{dx'} dx' \right\} \right] \delta(x, t) dx \\ & + \frac{d}{dt} \left( \frac{G}{2\pi(1 - \nu)} \frac{\partial \Phi}{\partial \delta} \int_{-L}^{+L} \left[ \int_{-L}^L \left\{ \frac{1}{(x - x')} \frac{d\delta(x', 0)}{dx'} dx' \right\} \right] \delta(x, t) dx \right) \end{aligned} \quad (27)$$

It can be noticed that unlike the force balance equations using Newtonian mechanics (Hirth and Lothe, 1983), equation (27) involves Thermodynamic State Index (TSI),  $\Phi$ , and its derivatives which relate Newtonian mechanics with the second law of thermodynamics. Equation (27) represents the most general form of threshold shear stress of dislocation at its incipient motion. The integral terms are identified in the following section, by applying suitable conditions.

## 6.2. Initial conditions of dislocation and derivation of threshold shear stress model

Identification of integral terms in equation (27) involves the application of initial condition. Initially, ( $t=0$ ), there is zero applied stress and hence, when the edge dislocation is at rest, the inertia term is equal to zero in equation (27). This can be identified by applying zero velocity condition for dislocation incipient motion as follows,

$$\frac{\partial \delta}{\partial t} = 0 \rightarrow \frac{\partial^2 \delta}{\partial t^2} = 0 \quad (28)$$

In this study, we investigate the non-dissipative processes of an edge dislocation incipient motion under thermo-mechanical loading. Thermally-induced (by preheating the test specimen) annihilation of a dislocation, represented by TSI,  $\Phi$  is a function of temperature. Hence, it is reasonable to neglect derivative terms,  $\frac{\partial \Phi}{\partial \delta}$  and  $\frac{\partial \Phi}{\partial \dot{\delta}}$  representing the evolution of TSI with strain and strain rate in equation (27). However, this latter assumption is invalid in the post-yield slip process. Therefore, neglecting the derivative terms of TSI,  $\Phi$  in equation (27) and combining with equation (28) gives the following simplified form,

$$\sigma_{DCS_{\theta}|t=0} = \frac{G(1 - \Phi)}{2\pi(1 - \nu)} \left[ \int_{-L}^L \left\{ \frac{1}{(x - x')} \delta' dx' \right\} \right] \quad (29)$$

Using the literature (Hirth and Lothe, 1983), it can be shown that the right-hand side of the equation (29) represents the following form,

$$\sigma_{DCS_{\theta}|t=0} = \sigma_{PN}(1 - \Phi) \quad (30)$$

where,  $\sigma_{PN}$  represents the Peierls-Nabarro model of at-rest slip resistance of a finite zone around the dislocation, formally known as Peierls-Nabarro stress (Hirth and Lothe, 1983). We have assumed that the dislocation geometry is unaltered during the incipient motion. Hence, the strain energy is independent of time (strain rate) and the  $\sigma_{PN}$  remain unchanged during elastic deformation. Therefore, using equation (27) and equation (30), we write the following equation for temperature-dependent threshold shear stress,

$$\sigma_{DCS\theta} = \alpha_{\theta} \rho_m \frac{d}{b} \int_{-L}^{+L} \delta'(x, t) \frac{\partial^2 \delta(x, t)}{\partial t^2} dx + \sigma_{PN}(1 - \Phi) \quad (31)$$

Equation (31) involves acceleration term,  $\frac{\partial^2 \delta(x, t)}{\partial t^2}$  inside an integral term, dislocation mass factor,  $\alpha_{\theta}$  and the TSI variable,  $\Phi$ . These model parameters are derived to get a workable model for threshold shear stress, in the following sections.

### 6.3. Derivation of model parameter: Acceleration of an edge dislocation

Numerically, it is shown (Oren et al., 2017) that the dislocation attains a stable terminal velocity through an acceleration process. However, no known experimental methods on the measurement of the acceleration of dislocation incipient motion in the elastic region of loading are found in the literature. Nevertheless, the dependence of dislocation terminal velocity on applied stress levels has been studied and reported in the literature (Tsuzuki et al., 2008). Hence, the dislocation has to undergo an acceleration process from a state of rest and the magnitude and period of acceleration are dependent on the applied strain rate. We consider that the acceleration term,  $\frac{\partial^2 \delta}{\partial t^2}$  in equation (31) is dependent on the applied strain rate. Based on the conservation of energy and momentum, a mathematical form can be derived for the acceleration and duration. The applied strain rate can be related to a terminal velocity of dislocation motion using Orowan's (Orowan, 1934) equation. Modified versions of the equation of dislocation terminal velocity (Orowan, 1934) are reported in the literature (Yaghoobi and Voyiadjis, 2018) to predict the dislocation velocity, leading to dislocation multiplication and subsequent plastic slip. Since we assume dominance of a non-dissipative process within the proportionality limit, we use the fundamental equation of dislocation velocity proposed by Orowan (Orowan, 1934), as follows,

$$v = \frac{\dot{\gamma}}{\rho b} \quad (32)$$

where,  $\rho$  and  $v$  represent the mobile dislocation density and average terminal velocity of dislocation, respectively.  $\dot{\gamma}$  represents the applied shear strain rate. Under applied strain rate, dislocation incipient motion initiates from a state of rest to a terminal velocity through an acceleration process. Since the current knowledge about the acceleration of dislocation in the elastic region of loading is limited, it is not possible to conclude that the dislocation accelerates uniformly or non-uniformly. However, for the sake of simplification, we assume that an average

value of dislocation acceleration can represent inertial force given in the integral term of the right-hand side of the equation (31). Hence, a timescale is introduced to represent the transient motion of dislocation within the proportionality limit, as follows,

$$\bar{a}(\dot{\gamma}) = \frac{\dot{\gamma}}{\rho b \tau} \quad (33)$$

where,  $\bar{a}$ ,  $\tau$  represents the average uniform acceleration and transient period of dislocation incipient motion, within the proportionality limit, respectively. Hence, by using equation (1) and equation (33) in equation (31), we get the following relation,

$$\sigma_{DCS_{\theta}} = \alpha_{\theta} \rho_m \frac{d \dot{\gamma}}{b \rho \tau} + \sigma_{PN}(1 - \Phi) \quad (34)$$

In practice, real-time measurement of the transient period,  $\tau$  defined in the current study, is difficult. Hence, a model for the transient period,  $\tau$  is derived to define an appropriate measure of temperature dependency of threshold shear stress,  $\sigma_{DCS_{\theta}}$ . Since the velocity and acceleration of dislocation is dependent on the applied strain rate (see equation (32) and equation (33)), we postulate that the average acceleration at two different strain rates can be related to the corresponding terminal velocity ratio as follows,

$$\frac{\bar{a}(\dot{\gamma})}{\bar{a}(\dot{\gamma}_0)} = \frac{f(v)}{f(v_0)} = h\left(\frac{v}{v_0}\right) \quad (35)$$

where,  $\dot{\gamma}_0$  and  $v_0$  represent reference strain rate and reference dislocation terminal velocity, respectively. Since the velocity of dislocation motion is influenced by thermal loading, temperature dependence is introduced to the proposed model of equation (35) as follows,

$$\frac{\bar{a}}{\bar{a}_0} = \left(\frac{v}{v_0}\right)^{q(\theta)} \quad (36)$$

where,  $\bar{a}_0$  and  $q(\theta)$  are the reference acceleration and acceleration rate exponent, respectively. Using equation (32) in equation (36), we get the following equation,

$$\frac{\bar{a}}{\bar{a}_0} = \left(\frac{\dot{\gamma}_0}{\dot{\gamma}}\right)^{-q(\theta)} \quad (37)$$

Substituting equation (33) in equation (37), we get the following equation,

$$\frac{\tau}{\tau_0} = \left( \frac{\dot{\gamma}}{\dot{\gamma}_0} \right)^{1-q(\theta)} \quad (38)$$

where,  $\tau_0$  represents a reference time-scale of dislocation acceleration. Representing  $p_\theta = 1 - q(\theta)$ , the transient period of dislocation incipient motion, within the proportionality limit, is given by the following equation,

$$\tau = \tau_0 \left( \frac{\dot{\gamma}}{\dot{\gamma}_0} \right)^{p_\theta} \quad (39)$$

Recent studies postulated that the dislocation may travel at speeds, higher than the shear wave velocity through the material (Pellegrini, 2014). However, in this study, we consider the limiting speed of the dislocation as the shear wave speed (Eshelby, 1953; Hirth and Lothe, 1983). Hence the maximum strain rate in our study is limited well below a value (order of  $10^4$ ) calculated from equation (32). Terminal velocity attained by a dislocation through an acceleration process has a varying mass (Eshelby, 1953; Ni, 2005) dependent on the acceleration (or applied strain rate). Hence, the mass of an accelerating dislocation is a function of the transient period. In this study, we use reference transient period,  $\tau_0$  which is derived based on Eshelby's model (Eshelby, 1953) for accelerating dislocation mass. Reference transient period is given by the following equation,

$$\tau_0 = \frac{d}{8c_0} \quad (40)$$

where,  $c_0$  represents the elastic wave speed through the medium. For a reference strain rate at which the inertial effects are negligible, the reference time scale is given by the equation (40). Hence, equation (34) is modified by using equation (39) and equation (40) to arrive at the following equation,

$$\sigma_{DCS_\theta} = \alpha_\theta \frac{8\dot{\gamma}_0 c_0 \rho_m}{b \rho} \left( \frac{\dot{\gamma}}{\dot{\gamma}_0} \right)^{1-p_\theta} + \sigma_{PN}(1 - \Phi) \quad (41)$$

It is to be noted that, equation (41) has an inertia term and strain energy term for the critical resistance. Temperature dependence of both the terms is not in similar form. Inertia term is affected by temperature in its mass, and strain energy term is influenced by the temperature through the Thermodynamic State Index.

#### 6.4. Derivation of model parameter: Dislocation mass at incipient motion

Dislocation activities in BCC metals like mild steel at low temperatures and low strain rates may be dominated by screw dislocations. However, edge dislocations are also active in high temperatures and high strain rate deformation of BCC metals. Since the equation (41) is derived for an edge dislocation, we use the mass conversion factor proposed by Weertman (Ni, 2005) for the mass of a screw dislocation. Mass of edge and screw dislocations are related (Ni, 2005) as follows,

$$m_{\text{edge}} = \left[ 1 + \left( \frac{c_2}{c_1} \right)^4 \right] m_{\text{screw}} \quad (42)$$

where,  $m_{\text{edge}}$  and  $m_{\text{screw}}$  are the masses of screw and edge dislocations. Wave speeds  $c_1$  and  $c_2$  are given by the following equations,

$$c_1 = \sqrt{\frac{\lambda + 2\mu}{\rho_m}} \quad (43)$$

$$c_2 = \sqrt{\frac{\mu}{\rho_m}} \quad (44)$$

where  $\lambda$  and  $\mu$  are the Lamé's parameters.

Dislocations annihilate at high temperatures (Suzuki et al., 1991). Annihilation of dislocations during the preheating of test specimens leads to a reduction in dislocation density. In this study, we consider the reference dislocation density at a test temperature,  $T=293\text{K}$ . Since, plasticity is out of the scope of the current study, dislocation annihilation due to strain-induced heating is not considered in this study. Many of the temperature-dependent models in the literature, successfully use an Arrhenius type function. In an Arrhenius type function, activation energy is the key parameter. Heat-induced annihilation of dislocations in metals is activated by the attainment of activation energy for the annihilation process. We introduce a similar form ( $\alpha_\theta = \text{constant} \times e^{f_1(T)}$ ) for dislocation mass at incipient motion,  $\alpha_\theta$ , by considering the exponential decline of proportionality limit stress, observed in experimental results (Blazynski, 2012; Campbell and Ferguson, 1970) for mild steel. It is well known that change in temperature in any metals causes a change in atomic vibrations. The amplitude of atomic vibrations increases with an increase in temperature. Such a change in atomic vibrations leads to change in the microstructure, such as a change in the dislocation density due to thermally activated annihilation

(Suzuki et al., 1991). In this study, we attempt to relate the change in dislocation density due to temperature change, with the amplitude of atomic vibrations in preheated specimens. Evolution of mean amplitudes of atomic vibration,  $u_\theta$  at different temperatures from experimental observation in mild steel (Owen and Evans, 1967) is used to relate mean amplitude of atomic vibration ( $\alpha_\theta = \text{constant} \times e^{f_2(u_\theta)}$ ). Hence, a decrease in dislocation density reduces average mass of dislocations from an initial value, at an elevated test temperature. Dislocation masses at incipient motion for reference temperature,  $\alpha_0$  and at given temperature,  $\alpha_\theta$  are related through corresponding mean amplitudes of atomic vibrations ( $\alpha_\theta = \alpha_0 e^{f_3(u_\theta, u_0)}$ ). Consecutively, the condition on equality of dislocation mass at the incipient motion for a reference temperature,  $\alpha_0$  and functional value of  $\alpha_\theta$  at a reference temperature is imposed ( $f_3(u_\theta, u_0) = f_3\left(\frac{u_\theta}{u_0}\right)$ ). Hence, we introduce an exponential form for the temperature-dependent mass factor,  $\alpha_\theta$ , which is given by the following equation,

$$\alpha_\theta = \alpha A_\theta e^{h_\theta \left(1 - \frac{u_\theta}{u_0}\right)} \quad (45)$$

where,  $A_\theta$  and  $h_\theta$  are temperature dependent material parameters.  $u_\theta$ ,  $u_0$  represents mean amplitudes of atomic vibration at a given temperature and reference temperature, respectively. Equation (41), equation (42), and equation (45) are used to get the functional form of the proposed model. Since equation (41) is derived for single dislocation, appropriate homogenization is required to derive the model for comparing the results of model prediction using equation (41) with the test data.

### 6.5. Homogenization of the model at continuum level RVE

Since the model is derived for single edge dislocation, homogenization of the model is done to represent Representative Volume Element (RVE), with the following assumptions. (i) The density of dislocation is uniform and they are assumed to be homogeneously distributed. Mechanical properties of metals are governed by the microstructure, such as dislocation density. In general practice, the material properties for a given mild steel test samples are assumed to be homogeneous and uniform. However, this assumption will be invalid when the standard deviations of the measurements for mechanical properties are considerably high, at various points of the sample. Hence, the assumption on the uniform and homogeneously distributed

dislocation density reasonably support the assumption on homogeneous material properties of mild steel, at an experimental level. (ii) Effect of neighboring dislocation, point defects, and long-range effects such as forest dislocations, grain boundaries, etc., are negligible on the dislocation incipient motion, within the proportionality limit. This assumption may be invalid for deformations at ultra-high strain rates, in which the boundary effects are not negligible. However, the present study is limited to a benchmark strain rate of  $10^4$  1/s, which well below the limiting strain rate at which the deformation speed reaches wave speed within the material. Hence, the assumption is valid for the present study. With the above assumptions, model predictions are averaged out for grain level representative volume element (RVE) from the derived microlevel dislocation model.

Experimental results on polycrystalline mild steel samples (Campbell and Ferguson, 1970) cannot be directly compared with the results obtained from the single grain-level RVE model. Critically resolved shear stress at grain level is scaled by Taylor's factor,  $M$ , to get proportionality limit stress of the bulk material under direct tensile loading (Shen et al., 2013). Taylor's factor can be estimated for a given sample by an experimental approach, like crystal orientation imaging technique or by a computational statistical averaging technique (Shen et al., 2013). In the present study, we assume that an average value of Taylor's factors for a given set of samples from the same batch of material can be used to predict proportionality limit stress of all the samples under direct tensile loading. Since information for the determination of Taylor's factor for the experimental samples (Campbell and Ferguson, 1970) are not available, we consider the fundamental relation of Taylor's factor,  $M$  (Taylor, 1938) with the critical shear stress and proportionality limit stress under direct tensile loading, as follows,

$$M = \frac{\sigma_{y_0}}{\sigma_{PN}} \quad (46)$$

where,  $\sigma_{y_0}$  represents the proportionality limit stress value of polycrystalline metals at low strain rates, under direct tensile loading, for which the inertial part of stress is negligible and  $\sigma_{PN}$  is represents the critically resolved shear stress at the crystal grain level. The value of Taylor's factor,  $M$  used in the current study are listed in Table 1. In equation (41), rate-independent part of grain level critical shear stress,  $\sigma_{PN}$  is estimated from the final form of equation (29) given in the literature (Hirth and Lothe, 1983), as follows,

$$\sigma_{PN} = \frac{2G}{(1-\nu)} \exp\left(-\frac{4\pi\zeta}{b}\right) \quad (47)$$

where,  $\zeta$  represents the half-width parameter of dislocation, given by the following equation,

$$\zeta = \frac{d}{2(1-\nu)} \quad (48)$$

Interplanar slip distance,  $d$  is given by the following equation,

$$d = a/\sqrt{h'^2 + k'^2 + l'^2} \quad (49)$$

where  $a$  represents lattice factor and  $h', k', l'$  represents slip plane direction cosines. An elasticity theory-based model for strain energy part of stress,  $\sigma_{PN}$  is given in equation (47). The second part of the right-hand side of equation (41) is replaced with equation (47). However, an appropriate estimate of the Thermodynamic State Index,  $\Phi$  is required for the model prediction. Using the laws of unified mechanics theory, Thermodynamic State Index,  $\Phi$  requires computation of entropy generation, as stated in equation (19). A model for entropy generation in dislocation-surrounding-system, due to thermal change, is derived in the following section.

## 6.6. Derivation of the entropy generation function

In this section, our objective is to model change in entropy, due to temperature change. To use the equation (41), Thermodynamic State Index (TSI),  $\Phi$  given in equation (19) has to be calculated. TSI is a function of change in entropy. Total change in entropy,  $\Delta s$  of a system, is the summation of internal entropy,  $\Delta s_i$  and entropy due to external sources,  $\Delta s_e$ . Considering dislocation as a system, the boundary of dislocation is defined by the surrounding atoms. Once the specimen is heated, atomic vibrations change. Such a change in atomic vibrations causes a change in the strain energy of dislocations. Hence, a part of heat energy,  $q$  carried by the surrounding atoms, is dissipated in reducing strain energy of dislocation. As described in section 2., we do not consider any change in the dislocation structure during mechanical tests. Thus, the total entropy change,  $\Delta s$  in dislocation is due to the change in atomic vibrations of the surrounding atoms, which is an external source of entropy. Hence, for a preheated specimen, change in entropy,  $\Delta s$  is given by the following equation,

$$\Delta s = \frac{\beta}{\rho_m \theta_0} \rho_m C_p (\theta - \theta_0) \quad (50)$$

where,  $C_p$  and  $\theta_0$  represents the specific heat capacity of the material and the reference temperature, respectively. The parameters,  $\rho_m$  and  $\theta$ , represents mass density and temperature, respectively. The term,  $\beta$  is the ratio between heat required to change the internal entropy in dislocation, leading to dislocation annihilation and heat required to increase the temperature of a specimen. While deriving equation (29) from equation (27), the entropy generation by internal heat generation due to strain and strain rate dependent processes are considered to be negligible, during the elastic deformation. Hence the total entropy generation is calculated from heat flux transfer as given in equation (50), due to change in kinetic energy of atoms. For temperatures lower than the reference temperature,  $\theta_0$ , the absolute value of change in entropy,  $\Delta s$  is used to calculate TSI. Experimental results are reported for lower yield stress (after the upper yield point representing proportionality limit) of mild steel (Campbell and Ferguson, 1970) and the proposed model in equation (41) predicts the proportionality limit stress, which is the upper yield point in case of mild steel. A proportionality factor,  $\ell_y$  is used to predict the lower yield stress values at different temperatures and strain rates. The factor,  $\ell_y$  is calculated as the ratio between lower and upper yield stresses from the test data for a given temperature and different strain rates. Values of temperature dependent rate exponent,  $p_\theta$  of the strain rate term in equation (41) are determined for three different sets of experimental data and a relationship is obtained for  $p_\theta$  in terms of a reference value,  $p_0$  and temperature to predict the values of  $p_\theta$  at different temperatures, as follows,

$$p_\theta = p_0 \frac{(\theta_m - \theta)}{(\theta_m - \theta_0)} \quad (51)$$

where,  $\theta_m$  represents the melting temperature of the material. The value of  $\beta$  is to be determined based on the thermodynamics of dislocation. For this, mechanism of thermally aided dislocation annihilation (Suzuki et al., 1991) is considered. Once the annihilation process is initiated, the strain energy level around the dislocation is reduced. A complete annihilation leads to zero strain energy. Life of a dislocation from its existence to complete annihilation due to preheating of the test specimen is defined by using an index, called Thermodynamic state index, (TSI)  $\Phi$ , which starts at zero and progresses to one (Basaran, 2020; Bin Jamal M. et al., 2020). TSI,  $\Phi = 1$  in

unified mechanics theory (Basaran, 2020; Bin Jamal M. et al., 2020), represents the completeness of the life of a system. In this study we consider preheating-induced dislocation annihilation from a reference state ( $\Phi = 0$ ) to a nearly annihilated state ( $\Phi = 0.99$ ), representing the validity of the strain energy equation of a dislocation, during the process. Strain energy of edge dislocation from the elasticity theory by Peierls-Nabarro model is given by the following equation (Hirth and Lothe, 1983),

$$\mathbb{E}_{\text{edge}} = \frac{G_{\theta} b^2}{4\pi(1-\nu)} \ln\left(\frac{r_u}{r_0}\right) \quad (52)$$

where,  $G_{\theta}$  is the shear modulus at a given temperature ( $\theta$ ),  $b$  is the Burgers vector and  $\nu$  is the Poisson's ratio.  $r_u$ ,  $r_0$  are the upper and lower integration bounds of dislocation in the radial direction, respectively. Generally, the value of  $r_u$  is of the order of the distance between two adjacent dislocations. Hence, the following expression is used to calculate the value of  $r_u$ .

$$r_u = \sqrt{1/\rho} \quad (53)$$

where  $\rho$  represents the dislocation density. To get a meaningful value for dislocation energy, it is suggested that the value of  $r_0$  shall be of the order of  $100b$  (Schoeck, 1995). Hence, the following equation is used to calculate the lower bound,  $r_0$  in equation (52),

$$r_0 = l_E b \quad (54)$$

where,  $l_E$  represents the energetic-zone coefficient. If equivalent energy given in equation (52), is supplied, the dislocation gets neutralized. Thermal specific energy supplied to the system can be written as,

$$q = \rho_m C_p \Delta\theta \quad (55)$$

where,  $C_p$  is the specific heat capacity of the material, and  $\rho_m$  is the mass density of the material. Change in temperature from a reference temperature is given by the following equation,

$$\Delta\theta = \theta - \theta_0 \quad (56)$$

By assuming that the dislocation core area is  $l_C b d$ , heat energy supplied to the dislocation from equation (55), is given by the following equation,

$$q_{\text{dis}} = l_C b d \rho_m C_p \Delta\theta \quad (57)$$

where  $l_c$  represents the dislocation geometry coefficient to account for an irregular dislocation geometry.

If thermal energy is supplied sufficiently to annihilate the dislocation, strain energy at the reference temperature reduces to zero. Hence, the following is relation valid, from equation (52) and equation (57) as follows,

$$\frac{G_0 b^2}{4\pi(1-\nu)} \ln\left(\frac{r_u}{r_0}\right) = l_c b d \rho_m C_p \Delta\theta_u \quad (58)$$

where,  $\theta_u$  represents the ultimate temperature at which the dislocation diffuses (thermally assisted core diffusion) and dislocation annihilate.  $G_0$  is the shear modulus at the reference temperature,  $\theta_0$ . Equation (58) is rearranged as follows,

$$\frac{G_0}{4\pi l_c \rho_m C_p (1-\nu)} \frac{b}{d} \ln\left(\frac{r_u}{r_0}\right) = \Delta\theta_u \quad (59)$$

From equation (56) and equation (59), we get the following equation,

$$\theta_u = \theta_0 + \frac{G_0}{4\pi l_c \rho_m C_p (1-\nu)} \frac{b}{d} \ln\left(\frac{r_u}{r_0}\right) \quad (60)$$

According to the unified mechanics theory (Basaran, 2020; Bin Jamal M. et al., 2020), when the temperature reaches annihilation temperature,  $\theta_u$ , TSI of dislocation reaches unity. Hence, the evolution of the dislocation annihilation process involves a change in entropy, at each test temperature. The Ultimate change in entropy for thermally assisted dislocation annihilation in preheated specimens can be written by using equation (50), as follows,

$$\Delta s_u = \beta C_p \left( \frac{\theta_u}{\theta_0} - 1 \right) \quad (61)$$

When entropy reaches its ultimate value, the TSI,  $\Phi$  tends to 0.99. Hence, from equation (19) for a value of  $\Phi_c = 1$ , we get the following,

$$4.606 \frac{R}{m_s} = \Delta s_u \quad (62)$$

Hence, from equation (61) and equation (62), we get the following equation,

$$\beta = \frac{4.606 R}{m_s C_p} \left( \frac{\theta_u}{\theta_0} - 1 \right)^{-1} \quad (63)$$

Using equation (53), equation (54), and equation (60) in equation (63), we get the following equation,

$$\beta = 4.606 \frac{R}{m_s} \frac{(4\pi l_c \rho_m \theta_0 (1 - \nu)) d}{G_0} \frac{1}{b} \left( \ln \left( \frac{\sqrt{1/\rho}}{l_E b} \right) \right)^{-1} \quad (64)$$

Using equation (64) in equation (50), the total change in entropy for thermally assisted dislocation annihilation is calculated. Hence, a complete form of equation (41) is obtained by using equation (45), equation (46), equation (47), equation (50), and equation (64). The derived model for continuum level predictions for the proportionality limit is used to compare with the test data of mild steel (Blazynski, 2012; Campbell and Ferguson, 1970) for a wide range of strain rates and temperatures.

## 7. Verification of the model prediction with test data

The proposed model in equation (41) is validated with experimental data for mild steel (Blazynski, 2012; Campbell and Ferguson, 1970). Values of strain at which the lower yield stress reported in the literature (Blazynski, 2012; Campbell and Ferguson, 1970) are very close to their corresponding proportionality limit stresses as shown in Fig. 1. In addition to that, the plastic strains at lower yield stresses are negligible. Hence, we calculate the average ratio between lower yield stresses and upper yield stresses, using test data shown in Fig. 1., and use the same factor to calculate lower yield stress using the proposed model in equation (41). By doing so, we assume based on experimental observations shown in Fig. 1., that, the effects of various dislocation mechanisms involved in the post-yield of mild steel are negligible at the lower yield point, where plastic strain is negligible. Screw dislocations dominate over edge dislocations in the deformation of mild steel. Hence, the mass of screw dislocations is calculated by using Weertman's (Ni, 2005) mass conversion factor. The energy of a screw dislocation is related to the energy of an edge dislocation (Hirth and Lothe, 1983) given in equation (52) as,  $E_{\text{screw}} = E_{\text{edge}}(1 - \nu)$ . Orowan's (Orowan, 1934) model given in equation (32) and the equation (64) necessitates quantification of initial mobile dislocation density. Estimation of total dislocation density from experimental observation is possible and segregation of them into mobile and

immobile dislocations, are reported in the literature, numerically (Wang et al., 2007) as well as analytically (Roters, 2003). However, an experimental procedure for the segregation of total dislocation density is not established under zero-load conditions. Nevertheless, mobile dislocation density is directly proportional to, and less than the total dislocation density (Voyiadjis and Abed, 2005). From numerical investigations (Wang et al., 2007), immobile dislocation density is found to be less than 1%. Hence, we assume that a reasonable range of total dislocation density represents the mobile dislocation density. Under these assumptions, we have listed the model parameters in Table 1. Dislocation geometry coefficient,  $l_C$  and energetic zone coefficient,  $l_E$  (of the order of  $100b$  (Schoeck, 1995)) can be obtained by using test data at two different temperatures and equation (41) and the value of the mass factor,  $\alpha$  and reference rate exponent,  $p_0$  can be obtained by using test data at reference temperature and equation (41). All other parameters listed in Table 1., are the fundamental quantities of mild steel.

$A_\theta$  in equation (45),  $p_0$  in equation (51) and  $\beta$  in equation (64) are determined by using test data (Campbell and Ferguson, 1970) at the reference temperature,  $\theta_0$  and equation (41). To calculate the value of  $h_\theta$  in equation (45), we consider the following conditions. At a limiting amplitude of vibration, for which the associated dislocation mass reduces to that for the core, the value of the mass factor,  $\alpha$  reduces to unity. We have assumed the limiting value of  $u_\theta$  in equation (45) as the mean amplitude of vibration at a temperature,  $\theta=1040$  K, which is about 75% of the melting temperature. Experimental values of the mean amplitude of atomic vibration (Owen and Evans, 1967) at different temperatures are listed in Table 2.

Table 1. Parameters used in the proposed model for mild steel

<u>Parameter</u>	<u>Symbol</u>	<u>Value</u>	<u>Unit</u>
Crystal structure	BCC		-
Lattice factor	a	$2.87 \times 10^{-10}$	m
Burgers vector	b	$2.48 \times 10^{-10}$	m
Young's modulus	E	$210 \times 10^9$	N/m <sup>2</sup>
Poisson's ratio	$\nu$	0.33	-

Mass density	$\rho_m$	7850.00	$\text{kg/m}^3$
Initial dislocation density (Brindley and Barnby, 1966)	$\rho$	$0.88 \times 10^{14}$	$\text{m/m}^3$
Reference strain rate	$\dot{\gamma}_0$	$2.66 \times 10^{-3}$	1/s
Taylor's factor	M	2.66	-
Mass factor	$\alpha$	$10^6$	-
Reference temperature	$\theta_0$	293	K
Melting temperature	$\theta_m$	1785	K
Mass decay coefficient	$A_\theta$	0.266	-
Energetic zone coefficient	$l_E$	150	-
Dislocation geometry coefficient	$l_C$	0.33	-
Specific heat capacity	$C_p$	510.8	J/kg-K
Molar mass	$m_s$	0.05497	kg/mol
Critical value of thermodynamic state index	$\Phi_c$	1.0	-
Rate exponent at the reference temperature	$p_0$	0.819	-

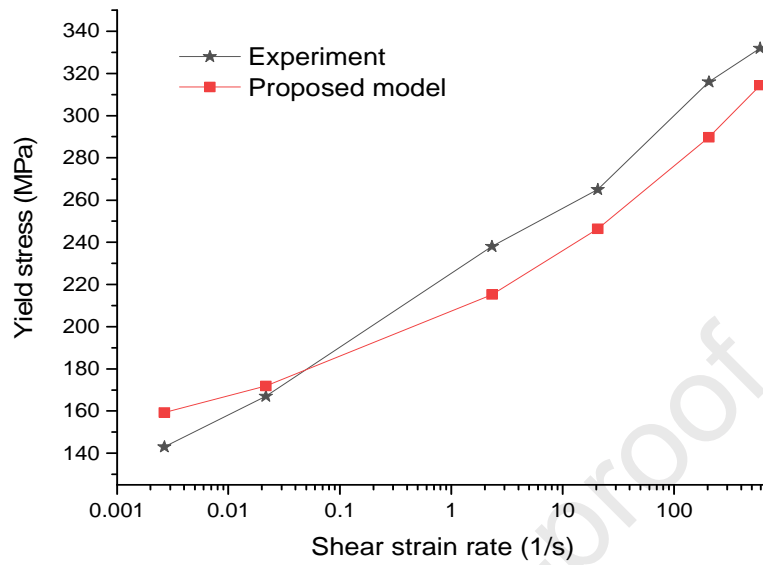


Fig. 4. Comparison between the proposed model and experimental results (Blazynski, 2012; Campbell and Ferguson, 1970) for mild steel at  $\theta=195$  K

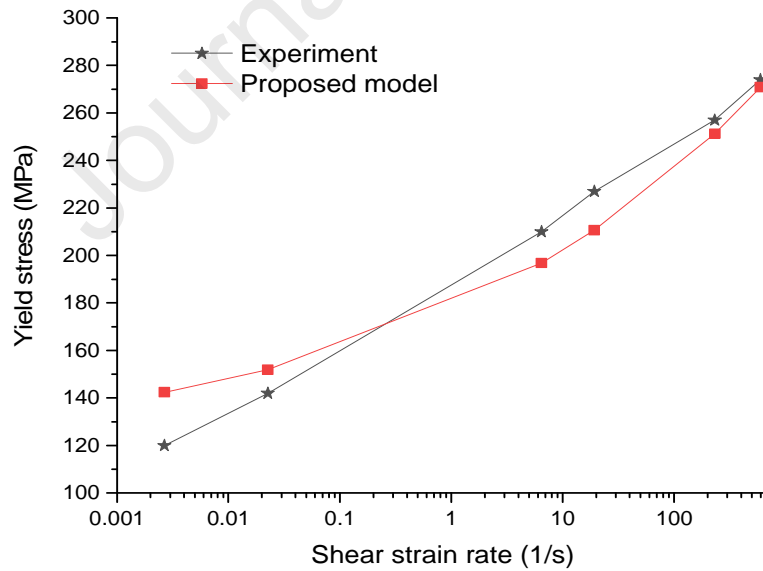


Fig. 5. Comparison between the proposed model and experimental results (Blazynski, 2012; Campbell and Ferguson, 1970) for mild steel at  $\theta=225$  K

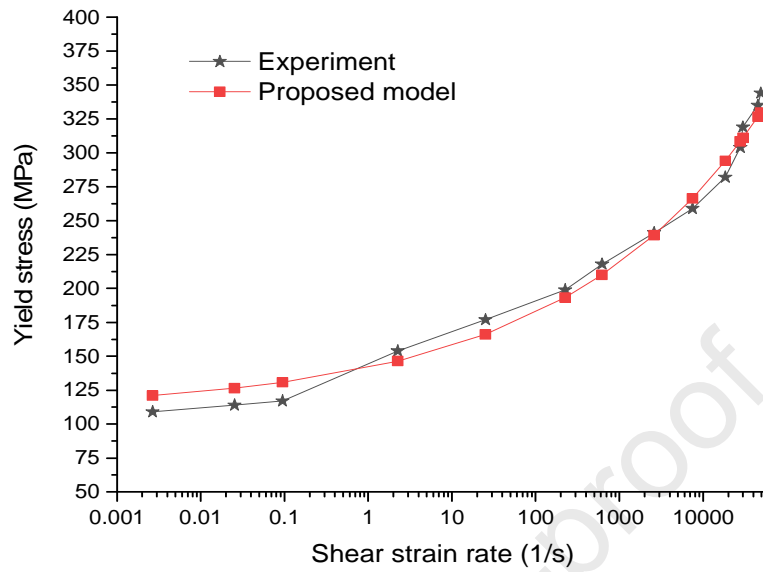


Fig. 6. Comparison between the proposed model and experimental results (Blazynski, 2012; Campbell and Ferguson, 1970) for mild steel at  $\theta=293$  K

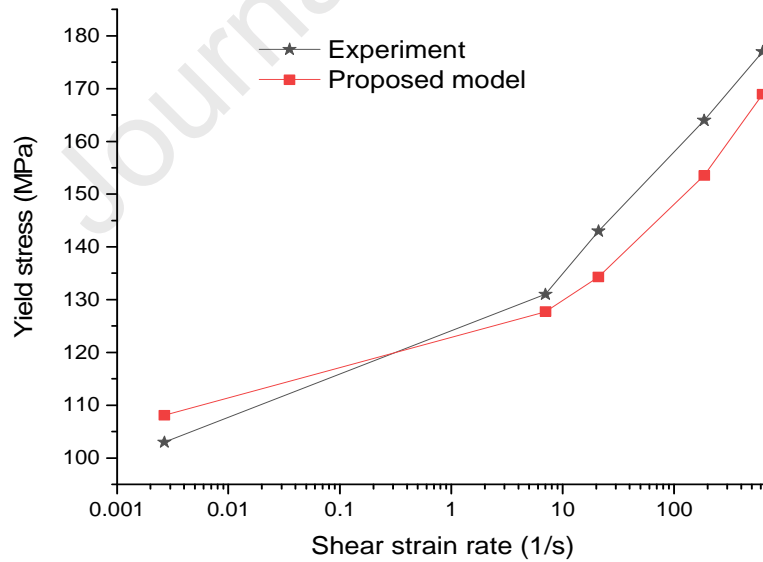


Fig. 7. Comparison between the proposed model and experimental results (Blazynski, 2012; Campbell and Ferguson, 1970) for mild steel at  $\theta=373$  K

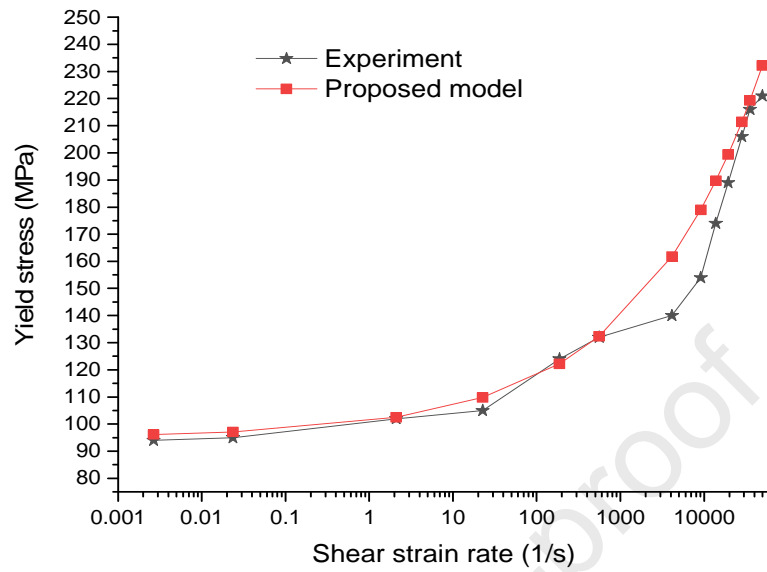


Fig. 8. Comparison between the proposed model and experimental results (Blazynski, 2012; Campbell and Ferguson, 1970) for mild steel at  $\theta=493\text{K}$

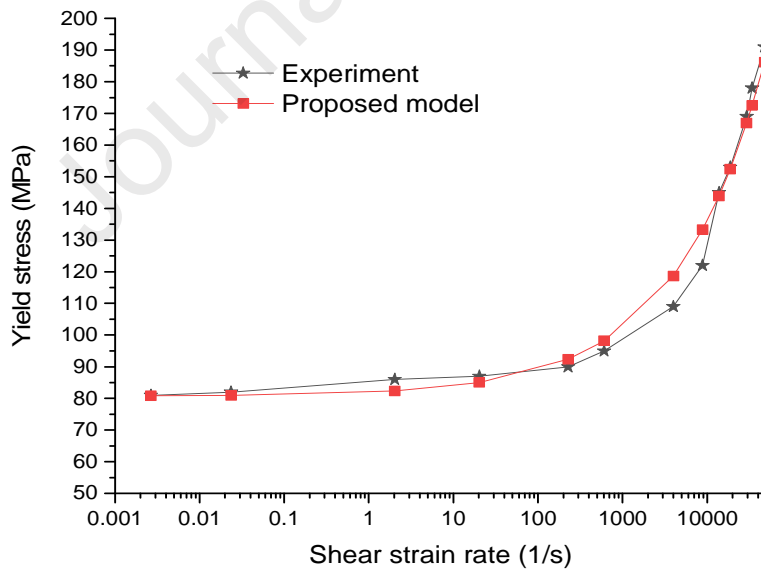


Fig. 9. Comparison between the proposed model and experimental results (Blazynski, 2012; Campbell and Ferguson, 1970) for mild steel at  $\theta=713\text{K}$

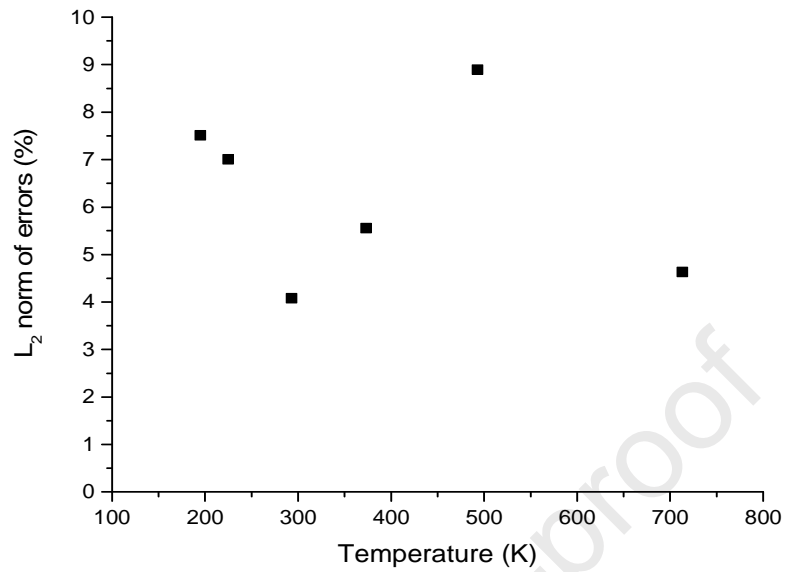


Fig. 10. Norm of relative errors in the model prediction at different temperatures

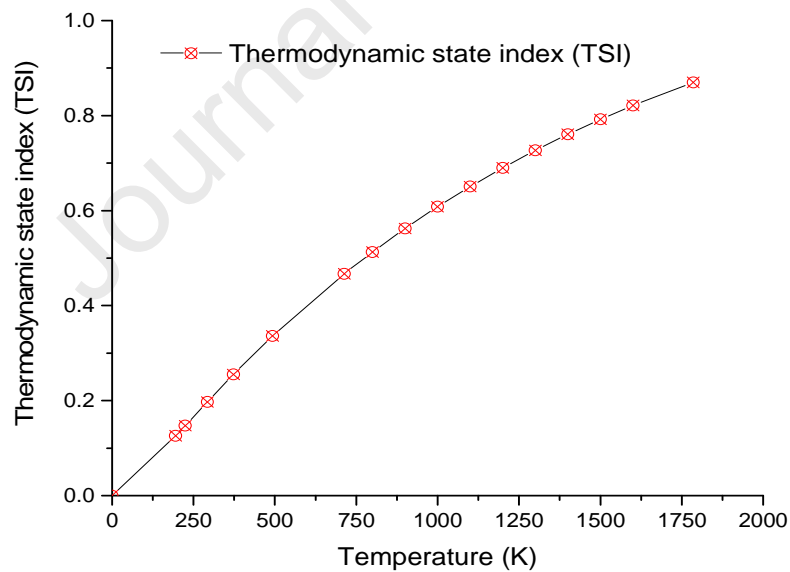


Fig. 11. Evolution of thermodynamic state index (TSI) with temperature

Table 2. Mean amplitudes of atomic vibration at different temperatures (Owen and Evans, 1967).

Temperature, $\theta$ (K)	195	225	293	373	493	713	1040
Mean amplitude of atomic vibration, $u_{\theta} (\times 10^{-10} \text{ m})$	0.0975	0.1035	0.1159	0.1291	0.1474	0.1783	0.2860

Fig. 4 through Fig. 9 shows that the model predictions at all the temperatures match well with the experimental data (Blazynski, 2012; Campbell and Ferguson, 1970).  $L_2$  norms of relative errors in the model predictions are plotted against temperature, as shown in Fig. 10, to assess scalar measures of error vectors whose components are calculated at different strain rates. Thermodynamic State Index (TSI) plotted in Fig. 11 represents a decrease in strain energy with an increase in temperature, leading to dislocation annihilation. It is shown in Fig. 11 that the external heat flux degrades the strain energy of dislocation at a faster rate at lower temperatures when compared with higher temperatures.

## 8. Comparison between proposed model predictions with Johnson-Cook model predictions

In this section, we attempt to compare the proposed thermodynamics-based model with that of an experimental curve-fit-based phenomenological model called the Johnson-Cook (J-C) model (Johnson and Cook, 1983). The proposed model in equation (41) is used to predict the proportionality limit stress of mild steel at different strain rates and temperatures (Blazynski, 2012; Campbell and Ferguson, 1970). Predictions using equation (41) are then scaled to get the lower yield stresses. Since, the ratio between lower yield stresses and proportionality limit stresses for mild steel shown in Fig.1., are found to be very close, we use an average value of the ratio between lower yield stress and proportionality limit stress to calculate the lower yield stress from the predictions for proportionality limit stress using equation (41). The scaled model predictions are then compared with the predictions using the J-C model (Johnson and Cook, 1983). J-C model is given by the following relation,

$$\sigma_y = [A + B (\bar{\epsilon}^P)^n] \left[ 1 + C \ln \left( \frac{\dot{\gamma}}{\dot{\gamma}_0} \right) \right] [1 - \theta^{*m}] \quad (65)$$

where, A, B, n, m, and C are the material parameters of the J-C model. The input variable,  $\bar{\epsilon}^P$  represents the magnitude of plastic strain. Since the values of strain at which proportionality

limit stress (before the onset of macrolevel plastic slip) and lower yield stresses are very close to each other,  $\bar{\epsilon}^p$  is set to zero. Value of dimensionless temperature coefficient,  $\theta^*$  in J-C model is given by the following equations (Johnson and Cook, 1983),

$$\theta^* = \frac{(\theta - \theta_0)}{(\theta_m - \theta_0)} \text{ when } \theta > \theta_0$$

$$\theta^* = 0 \text{ when } \theta \leq \theta_0$$

$$\theta^* = 1 \text{ when } \theta > \theta_m$$
(66)

Hence, the following equation is valid for predicting the proportionality limit stress.

$$\sigma_y = A \left[ 1 + C \ln \left( \frac{\dot{\gamma}}{\dot{\gamma}_0} \right) \right] [1 - \theta^{*m}]$$
(67)

It can be noted from the conditions given in equation (66) that, for all the temperatures below a reference temperature (293K in the current study), proportionality limit stress predictions for a given strain rate, are the same. Another major difference between the proposed model in equation (41) and the J-C model in equation (67), is the constant nature of the slope of the curve in equation number (67) with respect to  $\ln \left( \frac{\dot{\gamma}}{\dot{\gamma}_0} \right)$  for a given temperature. From equation (67), we get the following form for derivative with respect to  $\ln \left( \frac{\dot{\gamma}}{\dot{\gamma}_0} \right)$ ,

$$\frac{d}{d \ln \left( \frac{\dot{\gamma}}{\dot{\gamma}_0} \right)} (\sigma_y) = \ell_1$$
(68)

where,  $\ell_1$  is a constant term representing the right-hand side of the derivative of equation (67), for a given temperature. Using equation (41), the following form for derivative with respect to  $\ln \left( \frac{\dot{\gamma}}{\dot{\gamma}_0} \right)$  is obtained,

$$\frac{d}{d \ln \left( \frac{\dot{\gamma}}{\dot{\gamma}_0} \right)} (\sigma_{DCS_\theta}) = \ell_2 \exp \left( (1 - p_\theta) \ln \left( \frac{\dot{\gamma}}{\dot{\gamma}_0} \right) \right)$$
(69)

where,  $\ell_2$  represents a constant coefficient term in the right-hand side of the derivative of equation (41). Comparing the nature of derivatives in equation (68) (constant slope for an argument in  $\ln(\dot{\gamma})$ ) and equation (69) (exponentially varying slope for an argument in  $\ln(\dot{\gamma})$ ) with respect to that of experimental results plotted in Fig. 4 through Fig. 9 (nonlinear variation in

slope for an argument in  $\ln(\dot{\gamma})$ , the proposed model in equation (41) is very well capturing the rate and temperature dependence, observed in the test data (Blazynski, 2012; Campbell and Ferguson, 1970) for mild steel. We made an attempt to identify J-C material parameters using test data (Blazynski, 2012; Campbell and Ferguson, 1970), equation (67). J-C parameters are listed in Table 3. The parameters listed in Table 3 are used to demonstrate trends of J-C prediction and proposed model in equation (41) in comparison with test data (Blazynski, 2012; Campbell and Ferguson, 1970) for reference temperature as shown in Fig. 12.

Table 3. Johnson-Cook model parameters for test data (Blazynski, 2012; Campbell and Ferguson, 1970) of mild steel.

J-C parameter	Initial yield stress, A (N/m <sup>2</sup> )	Thermal softening coefficient, m	Strain rate hardening parameter, C
Value	$109.0 \times 10^6$	0.57	0.105

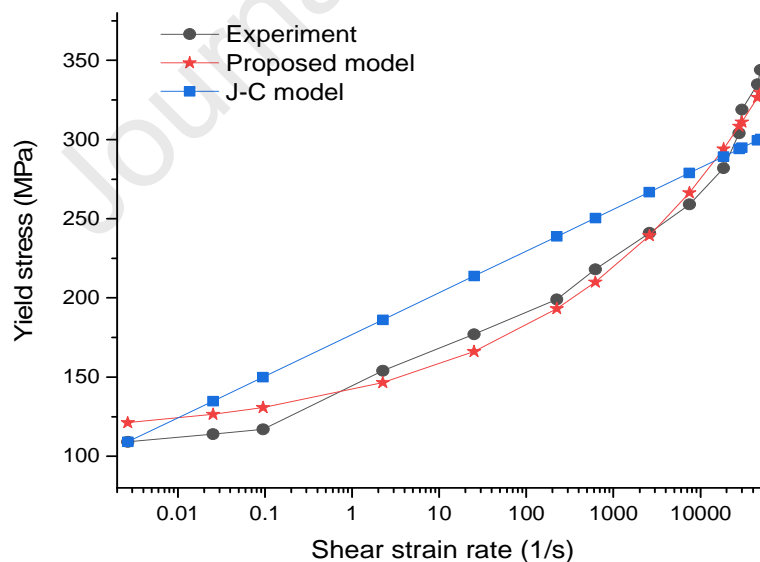


Fig. 12. Comparison between the proposed model and Johnson-Cook model (Johnson and Cook, 1983) with test data (Blazynski, 2012; Campbell and Ferguson, 1970) of mild steel at  $\theta=293$  K

Using equation (65) and equation (66), it is obvious that the trend line of J-C model prediction at the reference temperature is linear, as shown in Fig. 12. The proposed model predicts the trend of proportionality limit stress very well when compared with that of test data (Blazynski, 2012; Campbell and Ferguson, 1970) at the reference temperature.

## 9. Discussion

A micromechanics-based model for temperature dependent pre-yield dynamic response of mild steel is presented. We have shown that the dislocation inertia has to be included in the governing equation of motion of dislocations for modeling the high strain rate response of mild steel. Unlike commonly used macroscopic models (Johnson and Cook, 1983), the proposed formulation is derived from an idealized microlevel dislocation model, based on the postulated laws of mechanics. The proposed model is coupled with a rate-independent part by introducing strain energy of dislocation and rate-dependent part by introducing the kinetic energy of dislocation incipient motion. The proposed model suggests that the temperature effect is coupled with strain rate effects. Temperature dependence of rate-dependent part of the elastic response is modeled by introducing vibrational characteristics of the crystal lattice into the proposed model. Unified mechanics theory is used on the rate-independent part by stating the thermodynamics of strain energy evolution with temperature. Thermal effects on the geometrical parameters of dislocation and the acceleration of dislocation in the pre-yield regime are incorporated to capture the coupled effect of strain rate and temperature at the microlevel and under appropriate assumptions. Macrolevel scaling is done to compare the model prediction with test data (Blazynski, 2012; Campbell and Ferguson, 1970).

Dependence of inertial mass on the applied strain rate is introduced by using the transient period,  $\tau$  of dislocations. Since, the experimental data for the transient period of dislocation incipient motion in mild steel within the proportionality limit is not available in the literature, a phenomenological model is used to quantify it. The proposed power-law model is shown to be well capturing the trend of dynamic proportionality limit stress progression of mild steel at different strain rates when compared with J-C model predictions, as shown in Fig. 12.

The study presented here is limited to the development of a micromechanics-based model. Discussion on the determination of atomic vibrational amplitudes is out of the scope of this work. It is suggested that a molecular dynamics simulation may be used to get a measure of

temperature-dependent amplitudes of atomic vibrations with appropriate interatomic potentials. We have presented our model for mild steel for which the experimental data for amplitudes of atomic vibration are available in the literature (Owen and Evans, 1967).

The proposed proportionality limit stress prediction model is validated for a wide range of strain rates and temperature combinations. It is shown in Fig. 10. that the model prediction is matching well with the experimental data with an error bound of  $6.3\% \pm 1.8\%$ . Fig. 4 and Fig. 5 show much more linear variation in yield stress. Since the test temperatures for the results shown in Fig. 4 and Fig. 5 are below the reference temperature (293K), a similar linear trend can be obtained by using the J-C model. The proposed model is slightly off from the linear trend in prediction; however, the predicted results match very well with the test data. The nonlinear trends in prediction by the proposed model could be because, the temperature dependency in the kinetic energy term of the proposed model is incorporated by using an Arrhenius type exponential function in equation (41). The exponential function in equation (41), is used for evaluating the dislocation mass at incipient motion, as a function of amplitudes atomic vibration, for a given temperature. Hence, the predictions using the equation always show a nonlinear trend. Using equation (66) and equation (67), similar linearity is expected at the reference temperature, by the use of the J-C model. However, the test data at reference temperature (293K), as shown in Fig. 12, do not follow a linear trend as predicted by the J-C model. The essential features of the proposed model in equation (41), compared to the J-C model in equation (65) can be listed in terms of three major aspects. (i) The parameters in the proposed model, when compared with the J-C model, are fundamental quantities of atom and crystal. J-C model is derived by the experimental curve-fit procedure (Johnson and Cook, 1983) and hence the J-C model does not explicitly represent any micro-level or atomic level mechanism. (ii) It is easy to identify the material parameters in the J-C model by curve-fit to experimental data. Microlevel parameters such as dislocation density, transient period of dislocation, and atomistic parameters related to the crystal require sophisticated experiments. Nevertheless, the proposed model is shown to be predicting not only the test data but also their evolution with temperature and strain rate for mild steel, as shown in Fig. 6 through Fig. 9 and Fig. 12. (iii) Model inputs in the proposed equation (41) are microlevel and atomic-level parameters. J-C model in equation (65) doesn't have such micromechanics-based parameters. This is because, J-C model separates the effects of strain, strain rate, and temperature through the multiplicative decomposition of the

proportionality limit stress only at experimental length-scales. In this work, micro-level thermodynamics of an edge dislocation is used to derive a critical stress model. The proposed model requires calculation of entropy to explain the thermodynamic state of the material using the Thermodynamic State Index (TSI) axis.

## 10. Conclusions

- The temperature and strain rate-dependent dislocation mechanics based-model shows that dominance of inertial effects before the onset of observable plastic slip (within the proportionality limit) is a plausible hypothesis, that can explain the temperature and strain rate dependency of proportionality limit stress of mild steel.
- The model prediction matches very well with test data (Blazynski, 2012; Campbell and Ferguson, 1970) within an overall error bound of  $6.3\% \pm 1.8\%$  as shown in Fig. 10. Compared to the J-C model (Johnson and Cook, 1983), the proposed model predicts not only the values but also the trend of test data (Blazynski, 2012; Campbell and Ferguson, 1970), as shown in Fig. 12. This shows the accuracy in prediction by the proposed model, for mild steel.
- Critical shear stress in the proposed equation (41) in conjunction with Thermodynamic State Index (TSI) plotted in Fig. 11., exemplify the loss of strain energy of dislocation at high temperatures and the eventual annihilation of dislocations.

## References

- Ansart, J.P., Dornmeval, R., 1989. About the Strain Rate Dependence of Yield Stress and Flow Stress of Materials, in: *Advances in Plasticity*. Elsevier, pp. 371–374.  
<https://doi.org/10.1016/B978-0-08-040182-9.50093-X>
- Basaran, C., 2020. *Introduction to Unified Mechanics Theory with Applications*, 1st ed. Springer. <https://doi.org/10.1007/978-3-030-57772-8>
- Bin Jamal M., N., Kumar, A., Chebolu, L.R., Basaran, C., 2020. Low Cycle Fatigue Life Prediction Using Unified Mechanics Theory in Ti-6Al-4V Alloys. *Entropy* 1–31.  
<https://doi.org/10.20944/preprints201911.0317.v1>
- Blazynski, T.Z., 2012. *Explosive Welding, Forming and Compaction*.

- [https://doi.org/10.1016/0261-3069\(84\)90037-2](https://doi.org/10.1016/0261-3069(84)90037-2)
- Blazynski, T.Z. (Ed.), 1987. *Materials at High Strain Rates*. Springer Science & Business Media.
- Brandl, C., Derlet, P.M., Van Swygenhoven, H., 2009. Strain rates in molecular dynamics simulations of nanocrystalline metals. *Philos. Mag.* 89, 3465–3475.  
<https://doi.org/10.1080/14786430903313690>
- Brindley, B.J., Barnby, J.T., 1966. Dynamic strain ageing in mild steel. *Acta Metall.* 14, 1765–1780. [https://doi.org/10.1016/0001-6160\(66\)90028-9](https://doi.org/10.1016/0001-6160(66)90028-9)
- Campbell, J.D., Ferguson, W.G., 1970. The temperature and strain-rate dependence of the shear strength of mild steel. *Philos. Mag.* 21, 63–82. <https://doi.org/10.1080/14786437008238397>
- Eshelby, J.D., 1953. The equation of motion of a dislocation. *Phys. Rev.* 90, 248–255.  
<https://doi.org/10.1103/PhysRev.90.248>
- Hirth, J.P., Lothe, J., 1983. *Theory of Dislocations* (2nd ed.), 2nd ed, John Wiley & Sons, Inc. Krieger publishing company, malabar, Florida.
- Johnson, G.R., Cook, W.H., 1983. A constitutive model and data for metals subjected to large strains, high strain rates and high temperatures. *Proc. 7th Int. Symp. Ballist.*
- Ni, L., 2005. *The Effective Mass of an Accelerating Dislocation*. University of California.
- Oren, E., Yahel, E., Makov, G., 2017. Dislocation kinematics: A molecular dynamics study in Cu. *Model. Simul. Mater. Sci. Eng.* 25. <https://doi.org/10.1088/1361-651X/aa52a7>
- Orowan, E., 1934. Zur Kristallplastizität. III. *Zeitschrift für Phys.* 89, 605–613.  
<https://doi.org/10.1007/BF01341478>
- Owen, E.A., Evans, E.W., 1967. The variation with temperature of atomic vibration amplitudes in iron. *Br. J. Appl. Phys.* 18, 611–614. <https://doi.org/10.1088/0508-3443/18/5/309>
- Pellegrini, Y.-P., 2010. Dynamic Peierls-Nabarro equations for elastically isotropic crystals. *Phys. Rev. B* 81, 024101. <https://doi.org/10.1103/PhysRevB.81.024101>
- Pellegrini, Y.P., 2014. Equation of motion and subsonic-transonic transitions of rectilinear edge dislocations: A collective-variable approach. *Phys. Rev. B - Condens. Matter Mater. Phys.* 90, 1–18. <https://doi.org/10.1103/PhysRevB.90.054120>

- Polanyi, M., 1934. Lattice distortion which originates plastic flow. *Zeitschrift fur Phys.* 89, 660–664. <https://doi.org/10.1007/BF01341481>
- Roters, F., 2003. A new concept for the calculation of the mobile dislocation density in constitutive models of strain hardening. *Phys. Status Solidi Basic Res.* 240, 68–74. <https://doi.org/10.1002/pssb.200301873>
- Schoeck, G., 1995. The core energy of dislocations. *Acta Metall. Mater.* 43, 3679–3684. [https://doi.org/10.1016/0956-7151\(95\)90151-5](https://doi.org/10.1016/0956-7151(95)90151-5)
- Shen, J.H., Li, Y.L., Wei, Q., 2013. Statistic derivation of Taylor factors for polycrystalline metals with application to pure magnesium. *Mater. Sci. Eng. A* 582, 270–275. <https://doi.org/10.1016/j.msea.2013.06.025>
- Suzuki, T., Takeuchi, S., Yoshinaga, H., 2013. *Dislocation Dynamics and Plasticity*, Springer Science & Business Media.
- Suzuki, T., Takeuchi, S., Yoshinaga, H., 1991. High-Temperature Deformation of Metals and Alloys 120–156. [https://doi.org/10.1007/978-3-642-75774-7\\_8](https://doi.org/10.1007/978-3-642-75774-7_8)
- Taylor, G., 1992. Thermally-activated deformation of BCC metals and alloys. *Prog. Mater. Sci.* [https://doi.org/10.1016/0079-6425\(92\)90004-Q](https://doi.org/10.1016/0079-6425(92)90004-Q)
- Taylor, G.I., 1938. Plastic Strain in Metals. *J. Inst. Met.*
- Tsuzuki, H., Branicio, P.S., Rino, J.P., 2008. Accelerating dislocations to transonic and supersonic speeds in anisotropic metals. *Appl. Phys. Lett.* 92. <https://doi.org/10.1063/1.2921786>
- Vítek, V., 1968. Intrinsic stacking faults in body-centred cubic crystals. *Philos. Mag.* 18, 773–786. <https://doi.org/10.1080/14786436808227500>
- Voyiadjis, G.Z., Abed, F.H., 2005. Effect of dislocation density evolution on the thermomechanical response of metals with different crystal structures at low and high strain rates and temperatures. *Arch. Mech.* 57, 299–343.
- Wang, Z.Q., Beyerlein, I.J., LeSar, R., 2007. The importance of cross-slip in high-rate deformation. *Model. Simul. Mater. Sci. Eng.* 15, 675–690. <https://doi.org/10.1088/0965-0393/15/6/006>

Yaghoobi, M., Voyiadjis, G.Z., 2018. The effects of temperature and strain rate in fcc and bcc metals during extreme deformation rates. *Acta Mater.* 151, 1–10.  
<https://doi.org/10.1016/j.actamat.2018.03.029>

Journal Pre-proof

## Highlights

**Title: A unified mechanics theory-based model for temperature and strain rate dependent proportionality limit stress of mild steel**

**Authors: Noushad Bin Jamal M<sup>a</sup>, C. Lakshmana Rao<sup>a</sup>, and Cemal Basaran<sup>b</sup>**

<sup>a</sup>*Department of Applied Mechanics, Indian Institute of Technology, Madras 600036.*

<sup>b</sup>*Civil, Structural and Environmental Engineering, University at Buffalo, State University of New York.*

**Following are the highlights of this research manuscript.**

- An Energy based approach to derive the governing equation of motion of an edge dislocation
- Inertia dominant mechanism to capture strain rate dependence in metals.
- A unified mechanics theory (unification of laws of Newton and thermodynamics)-based model for temperature dependence of the elastic limit stress.
- Pre-yield dynamic strengthening is predicted using the proposed analytical model.

**Declaration of interests**

The authors declare that they have no known competing financial interests or personal relationships that could have appeared to influence the work reported in this paper.

The authors declare the following financial interests/personal relationships which may be considered as potential competing interests:

Journal Pre-proof